

Cure Kinetics of the Ring-Opening Metathesis Polymerization of Dicyclopentadiene

M. R. KESSLER,¹ S. R. WHITE²

¹Department of Mechanical Engineering, the University of Tulsa, Tulsa, Oklahoma

²Department of Aeronautical and Astronautical Engineering, University of Illinois at Urbana–Champaign, Urbana–Champaign, Illinois

Received 22 February 2002; accepted 16 April 2002

ABSTRACT: The cure kinetics of polydicyclopentadiene prepared by ring-opening metathesis polymerization with three different concentrations of Grubbs' catalyst were examined with differential scanning calorimetry. The experimental data were used to test several different phenomenological kinetic models. The data were best modeled with a model-free isoconversional method. This analysis revealed that the activation energy increased significantly for degrees of cure greater than 60%. The catalyst concentration had a large effect on the cure kinetics. © 2002 Wiley Periodicals, Inc. *J Polym Sci Part A: Polym Chem* 40: 2373–2383, 2002

Keywords: activation energy; dicyclopentadiene; differential scanning calorimetry (DSC); kinetics (polym.); ROMP

INTRODUCTION

Polydicyclopentadiene (pDCPD) is generally a highly crosslinked polymer of high toughness formed by a ring-opening metathesis polymerization (ROMP) of its monomer precursor. The polymerization is highly exothermic because of the relief of ring strain energy and can be initiated by transition-metal/alkylidene complexes. A recently developed ruthenium-based catalyst (Grubbs' catalyst) shows high metathesis activity and tolerance of a wide range of functional groups as well as oxygen and water.¹

The polymerization of dicyclopentadiene (DCPD) with Grubbs' catalyst in reaction injection molding (RIM) and resin transfer molding (RTM) applications results in a polymer with excellent mechanical properties and little chemical

shrinkage.² Recently, White et al.³ reported on a material system that incorporates DCPD and Grubbs' catalyst into an epoxy matrix to automatically repair the material when it is damaged. Similarly, Kessler and White⁴ used DCPD to repair delamination damage in laminate composites in which Grubbs' catalyst was embedded in the matrix of the composite material.

In self-healing applications, the polymerization kinetics determine the extent to which polymerization can occur for a given time and at a particular temperature and, therefore, the healing efficiency. In RIM and RTM applications, the kinetics influence the thermochemical history of the part, ultimately dictating the processing time and final physical properties. Modeling the cure kinetics of DCPD and Grubbs' catalyst has utility not only in optimizing self-healing materials but also in processing RIM/RTM-fabricated pDCPD.

In phenomenological modeling of the cure kinetics of thermosetting polymers, an internal state variable is defined to which all other properties are related. This state variable is the de-

Correspondence to: M. R. Kessler (E-mail: mrk@mikekessler.net)

Journal of Polymer Science: Part A: Polymer Chemistry, Vol. 40, 2373–2383 (2002)
© 2002 Wiley Periodicals, Inc.

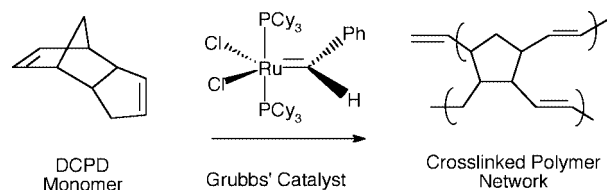


Figure 1. ROMP of DCPD with Grubbs' catalyst.

gree of cure (α) and ranges from 0 (uncured) to 1 (fully cured). Thermal analysis by differential scanning calorimetry (DSC) is the most commonly used experimental technique to determine the cure kinetics of thermosets.⁵ For DSC measurements, the degree of cure is defined as

$$\alpha(t) = \frac{H(t)}{H_R} \quad (1)$$

where $H(t)$ is the enthalpy of reaction up to time t and H_R is the total enthalpy of reaction. DSC provides a continuous history of the heat evolved during polymerization, which can then be integrated to yield $H(t)$, and through eq 1, the degree of cure history is obtained.

Traditionally, the determination of kinetic parameters from DSC measurements is accomplished with isothermal data.⁵ Isothermal measurements do have the advantage of a complete separation between the variables of time and temperature. However, a significant advancement of the cure state can take place before DSC can reach and stabilize at the desired temperature, and at low temperatures, the reaction may not proceed to completion. Alternatively, dynamic data allow for a better capture of the kinetics at both the start and end of a reaction, and complex reaction mechanisms can be more easily interpreted by a comparison of measurements at different heating rates.

In this study, a phenomenological cure kinetics model was developed from dynamic DSC data of DCPD cured with Grubbs' catalyst over a range of catalyst concentrations. The experimental data were used to test several different phenomenological kinetic models over a range of heating rates, from 2 to 15 °C min⁻¹.

MATERIALS AND METHODS

Materials

DCPD monomer stabilized with 100–200 ppm *p*-*tert*-butylcatechol was purchased from Acros Or-

Table 1. Three Catalyst Concentrations Analyzed

Designation	Catalyst (g)/DCPD (mL) ^a	Catalyst Molecules/DCPD Molecules ^b
Low	1.33×10^{-3}	1:5000
Medium	2.00×10^{-3}	1:3750
High	2.67×10^{-3}	1:2500

^a The Density of DCPD was 1.0710 g/cm³.

^b The molecular weights of DCPD and the catalyst were 132.2 and 822.96, respectively.

ganics (Geel, Belgium). As supplied, the monomer was predominantly endo isomer. The monomer was purified by low-vacuum distillation for the removal of any trace impurities. Bis(tricyclohexylphosphine)benzylidene ruthenium(IV) dichloride (Grubbs' catalyst) was purchased from Strem Chemicals (Newburyport, MA) in the form of a fine, purple powder. The catalyst was stored and prepared in a glove box with N₂ purge for the minimization of decomposition over time.

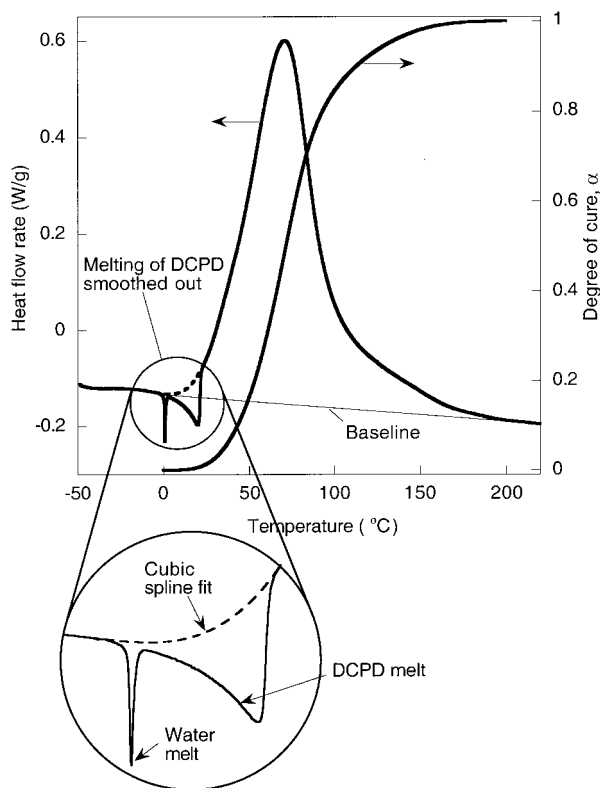


Figure 2. Typical DSC scan (at 5 °C/min) and corresponding degree of cure history (1:3750 catalyst concentration).

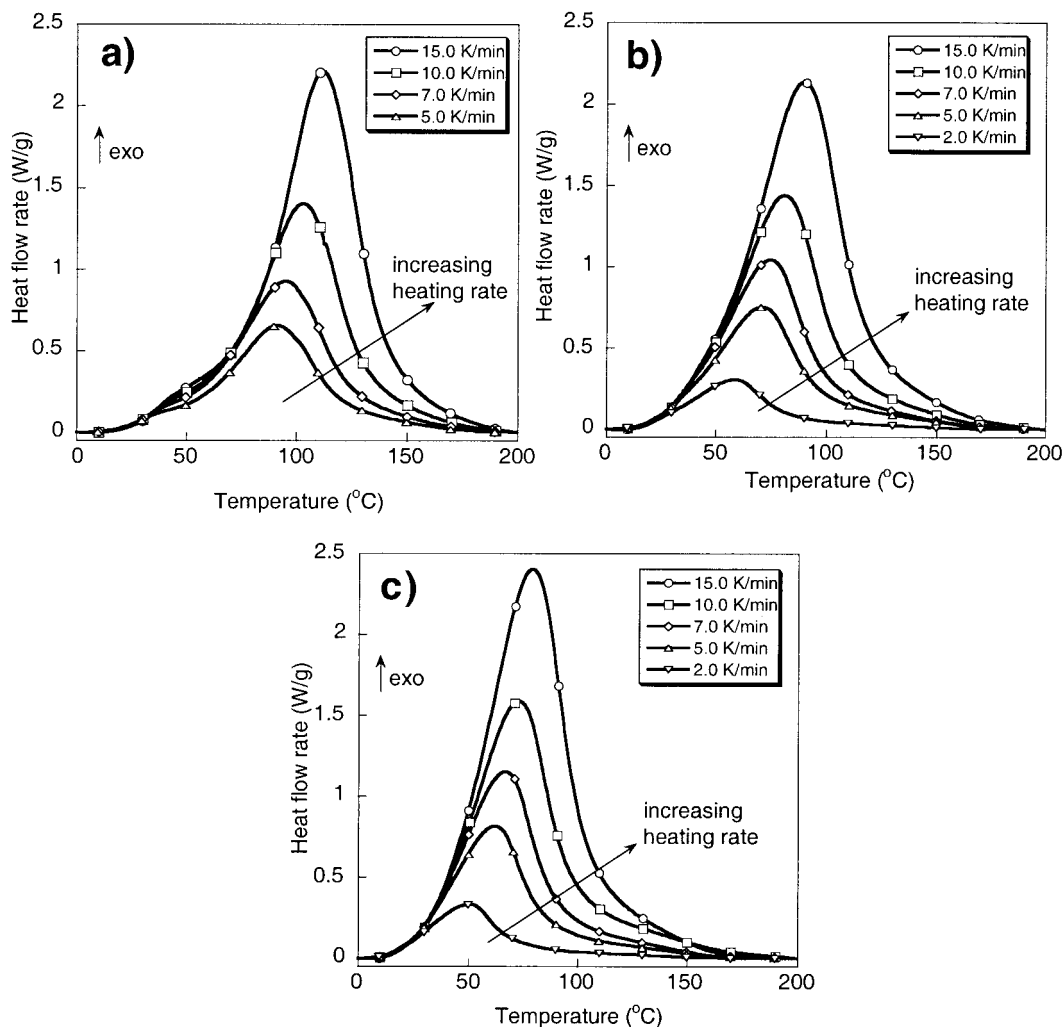


Figure 3. DSC curves for (a) low-concentration, (b) medium-concentration, and (c) high-concentration DCPD and Grubbs' catalyst samples.

The mixing of DCPD with Grubbs' catalyst initiates the ROMP reaction shown in Figure 1. This ROMP reaction can be extremely rapid at room temperature, the speed depending on the catalyst concentration and sample size. The polymerization of DCPD was accomplished with three different catalyst/monomer ratios, as shown in Table 1.

Technique

Vials containing 20, 30, or 40 mg of catalyst and a small Teflon-coated magnetic stir bar were placed in a water bath at 15 °C. To each was added 15 mL of distilled DCPD, also cooled to 15 °C, and the solutions were mixed vigorously with the magnetic stirrer for about 30 s, by which time the catalyst powder had dissolved and a homoge-

neous solution was achieved for the three concentrations listed in Table 1. The vials were then immediately placed in liquid nitrogen for flash freezing of the solution and were stored in a -80 °C freezer. We prepared a typical DSC sample by removing a small amount of the frozen solution and placing it in an aluminum DSC pan, weighing the sample, and loading it into the DSC chamber at a standby temperature of -5 °C. The average and standard deviations in sample size were 9.8 and 1.9 mg, respectively.

DSC measurements were performed with a Mettler Toledo DSC821^e connected to a computer equipped with STAR^e (version 6.0) evaluation software for the manipulation and transfer of data. The DSC cell was swept by a constant flow of nitrogen at 80 mL min⁻¹. The DSC was first

Table 2. Sample Size and Measured Total Enthalpy of Reaction

Concentration	Heating Rate (°C/min)	Sample Size		Total Enthalpy of Reaction (J/g)
		Initial (mg)	Final (mg)	
Low	15	9.3	8.9	456.7
	10	10.3	9.8	459.9
	7	8.3	8.1	453.5
	5	7.8	7.4	443.5
Medium	15	9.1	8.9	463.8
	10	6.3	6.1	457.3
	7	7.2	7.1	461.6
	5	11.6	11.3	478.8
	2	12.6	12.3	436.8
High	15	11.2	11.2	472.6
	10	10.8	10.7	485.3
	7	11.9	11.9	474.1
	5	11.1	11.1	467.5
	2	10.3	10.2	442.6

calibrated in duplicate for temperature and heat flow accuracy with indium, water, octane, and zinc standards. Tests were performed on the DCPD/catalyst system in a dynamic mode at various heating rates over a temperature range of -50 – 250 °C. Data obtained at heating rates of 2, 5, 7, 10, and 15 °C · min⁻¹ were converted into ASCII format, and kinetic analysis was performed with the Netzsch Thermokinetics program (version 2001.2), Mathematica (version 4.1.1), and standard statistical and plotting programs.

CURE KINETIC MODELING

Model-Fitting Method

In kinetic analysis, it is generally assumed that the rate of reaction can be described by two separable functions, $K(T)$ and $f(\alpha)$, such that

$$\frac{d\alpha}{dt} = K(T) \cdot f(\alpha) \quad (2)$$

where $d\alpha/dt$ is the rate of reaction, $K(T)$ is the temperature-dependent rate constant, and $f(\alpha)$ corresponds to the reaction model. The temperature dependence of the reaction rate is commonly described by the Arrhenius equation:

$$K(T) = A \cdot \exp\left(\frac{-E}{RT}\right) \quad (3)$$

where R is the universal gas constant, E is the activation energy, and A is the pre-exponential factor.

For experiments in which samples are heated at a constant rate, the explicit time dependence in eq 2 can be eliminated so that

$$\frac{d\alpha}{dT} = \frac{A}{\beta} \cdot \exp\left(-\frac{E}{RT}\right) \cdot f(\alpha) \quad (4)$$

Table 3. Reaction Models Evaluated

Reaction Model	Model Designation	$f(\alpha)$	Parameters
First order	F1	$(1 - \alpha)$	A, E
Second order	F2	$(1 - \alpha)^2$	A, E
n th order	F n	$(1 - \alpha)^n$	A, E, n
n th order with autocatalysis	C n	$(1 - \alpha)^n(1 + K_{\text{cat}}\alpha)$	A, E, n, K_{cat}
Prout–Tompkins equation (autocatalytic)	PT	$(1 - \alpha)^n\alpha^m$	A, E, n, m

Table 4. Results of Multiple Linear Regression Analysis

Catalyst Concentration	Model Designation	log[A] (s ⁻¹)	<i>E</i> (kJ/mol)	<i>n</i>	<i>K</i> _{cat}	<i>m</i>	Correlation Coefficient
Low	F1	4.961	51.31	—	—	—	0.9822
	F2	8.563	75.69	—	—	—	0.9788
	Fn	6.199	59.65	1.328	—	—	0.9864
	Cn	4.409	48.76	1.616	0.436	—	0.9917
	PT	5.653	55.50	1.335	—	0.093	0.9865
Medium	F1	4.698	46.55	—	—	—	0.9815
	F2	8.083	67.97	—	—	—	0.9921
	Fn	7.019	61.21	1.671	—	—	0.9934
	Cn	5.281	51.10	1.927	0.365	—	0.9965
	PT	5.899	53.27	1.668	—	0.168	0.9942
High	F1	5.240	48.59	—	—	—	0.9757
	F2	8.834	70.86	—	—	—	0.9938
	Fn	8.657	69.76	1.948	—	—	0.9938
	Cn	6.649	58.16	2.192	0.370	—	0.9966
	PT	7.230	60.02	1.923	—	0.176	0.9947

where $\beta = dT/dt$ is the heating rate.

A multivariate version of the Borchardt and Daniels method⁶ is frequently used in the evaluation of dynamic DSC data. In this method, the kinetic parameters (*A* and *E*) are obtained by a linearizing transformation of eq 4 so that

$$\ln \frac{d\alpha/dT}{f(\alpha)} = \ln \left(\frac{A}{\beta} \right) - \frac{E}{RT} \quad (5)$$

This linear equation, which has the form $y = a_0 + a_1x$ with $x = 1/T$, can be used to determine the optimal fit of the kinetic parameters by multiple linear regression.

Model-Free Isoconversional Method

The model-free isoconversional method assumes that both the activation energy and pre-exponential factor are functions of the degree of cure. The activation energy is determined by Friedman's method⁷ from the logarithmic form of the rate equation for each heating rate:

$$\ln[\beta_i(d\alpha/dT)_{\alpha,i}] = \ln[A_\alpha f(\alpha)] - \frac{E_\alpha}{RT_{\alpha,i}} \quad (6)$$

where the subscript α is the value at a particular degree of cure and *i* refers to data from a given heating rate experiment. The activation energy at each degree of cure is calculated with linear regression from a plot of $\ln[\beta_i(d\alpha/dT)_{\alpha,i}]$ versus

$1/T_{\alpha,i}$ (Friedman plot) across all of the heating rates tested. Similarly, the product of the cure-dependent pre-exponential factor and the reaction model can be obtained from the *y* intercept of the Friedman plot. These parameters can alternately be calculated by an integral isoconversional method described by Flynn and Wall⁸ and Ozawa.⁹

The isoconversional approach can be used to evaluate both simple and complex chemical reactions. For the evaluation of data with this method, no kinetic rate expression is assumed *a priori*.

RESULTS

A typical DSC scan and the corresponding degree of cure are shown in Figure 2. When the scan begins at -50 °C, the sample is a frozen solid. Near -5 °C, a broad endothermic peak begins and extends from -5 to 15 °C. This endothermic peak corresponds to the melting of DCPD. Superimposed on this melting transition is a sharp endothermic peak at 0 °C corresponding to the presence of water in the sample, presumably condensation resulting from the flash freezing of the sample in liquid nitrogen immediately after mixing. Analyzing the size of the peak and assuming 2400 J g^{-1} for ΔH of water, we determined the total content of water to be less than 0.005% for all samples analyzed. Later tests on samples that were not flash-frozen showed no endothermic

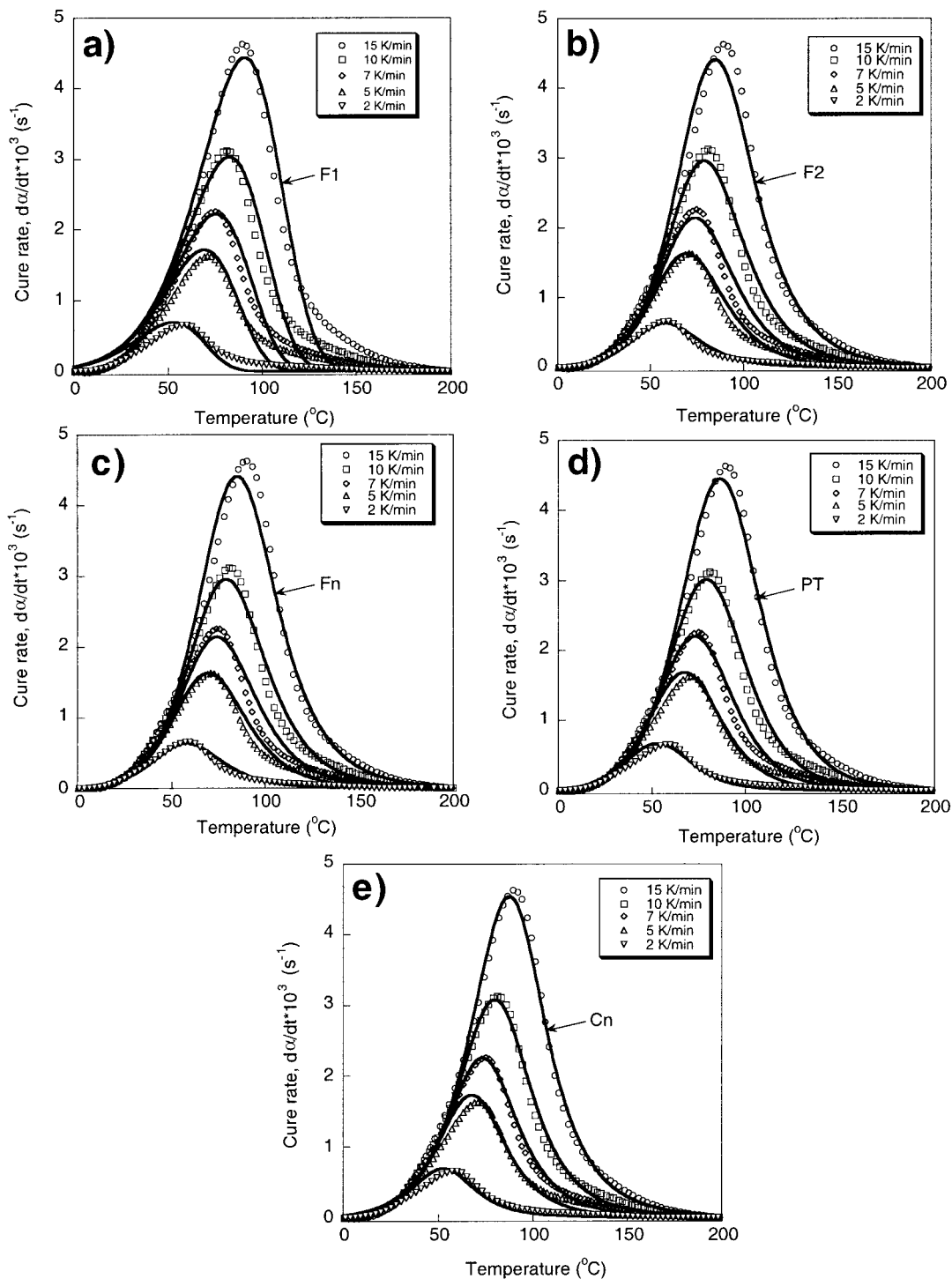


Figure 4. Model fits of DSC data for the medium catalyst concentration: (a) first order (F1), (b) second order (F2), (c) n th order (Fn), (d) expanded Prout-Tompkins (PT), and (e) n th order with autocatalysis (Cn).

melting peak at 0 $^{\circ}\text{C}$ but otherwise were identical to those that were flash-frozen. To correct for these melting transitions in the evaluation of the degree of cure, we constructed a best fit spline

connecting the premelt and postmelt regions (the dashed line in Fig. 2) to effectively eliminate the melting phenomenon from the heat flow curves. As a justification, less than 0.5% of cure advance-

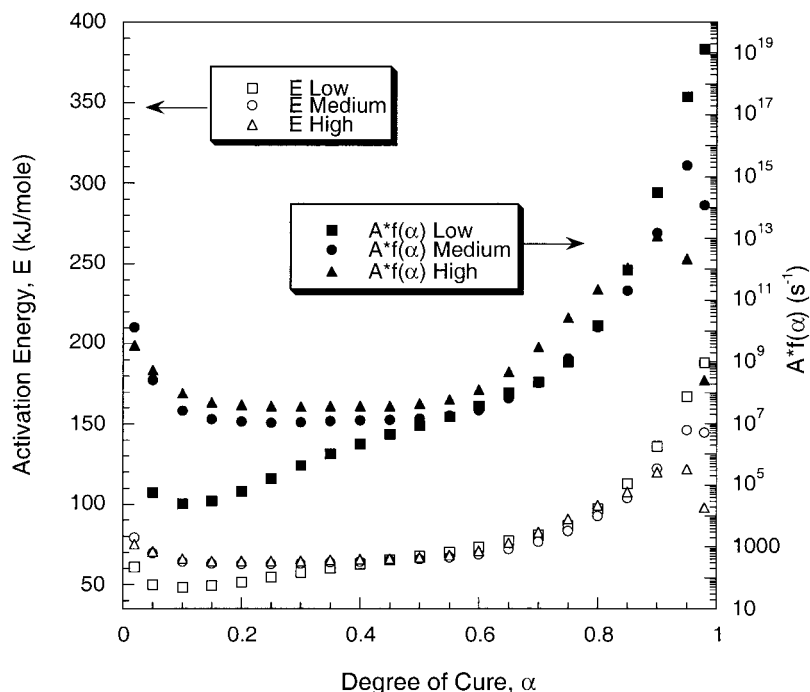


Figure 6. Model-free results for the activation energy and product $A \times f(\alpha)$ versus the degree of cure for all three catalyst concentrations.

To determine a model-free estimation for the activation energy, we first created a Friedman plot with the logarithmic form of the rate equation (eq 6) for all of the heating rates. A Friedman plot for the medium catalyst concentration is shown in Figure 5. The activation energy and product of $A \times f(\alpha)$ at each degree of cure were calculated by linear regression at a specific value

of α . The straight lines in Figure 5 correspond to these linear fits for α values ranging from 0.02 to 0.98.

The complex dependence of the activation energy on the degree of cure can be seen in Figure 6 for all three catalyst concentrations. It is immediately apparent that the activation energy increases significantly for all three concentrations after the degree of cure reaches about 0.6 and especially near the end of cure. The assumption of a constant activation energy (as is the case for all of the reaction models listed in Table 4) is reasonable up to this critical degree of cure but too restrictive for the entire cure range. One interpretation of this behavior is an apparent decrease in molecular mobility as the degree of cure increases above 0.6 and the polymer gels. It is also apparent that the activation energies for all three catalyst concentrations are quite comparable. Finally, the plot of the product of $\ln[A \times f(\alpha)]$ appears to vary similarly to the activation energy with the degree of cure. This correspondence is due to the isokinetic relationship^{7,12} or the kinetic compensation effect,¹³ which suggests that the value of $\ln A_\alpha$ varies linearly with E_α . Such a relationship has been observed in the curing and decomposition of numerous other polymer systems.^{14–17}

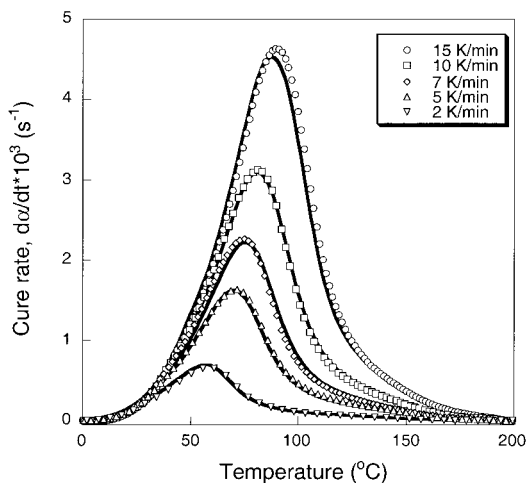


Figure 7. Model-free prediction and experimental results for the medium catalyst concentration.

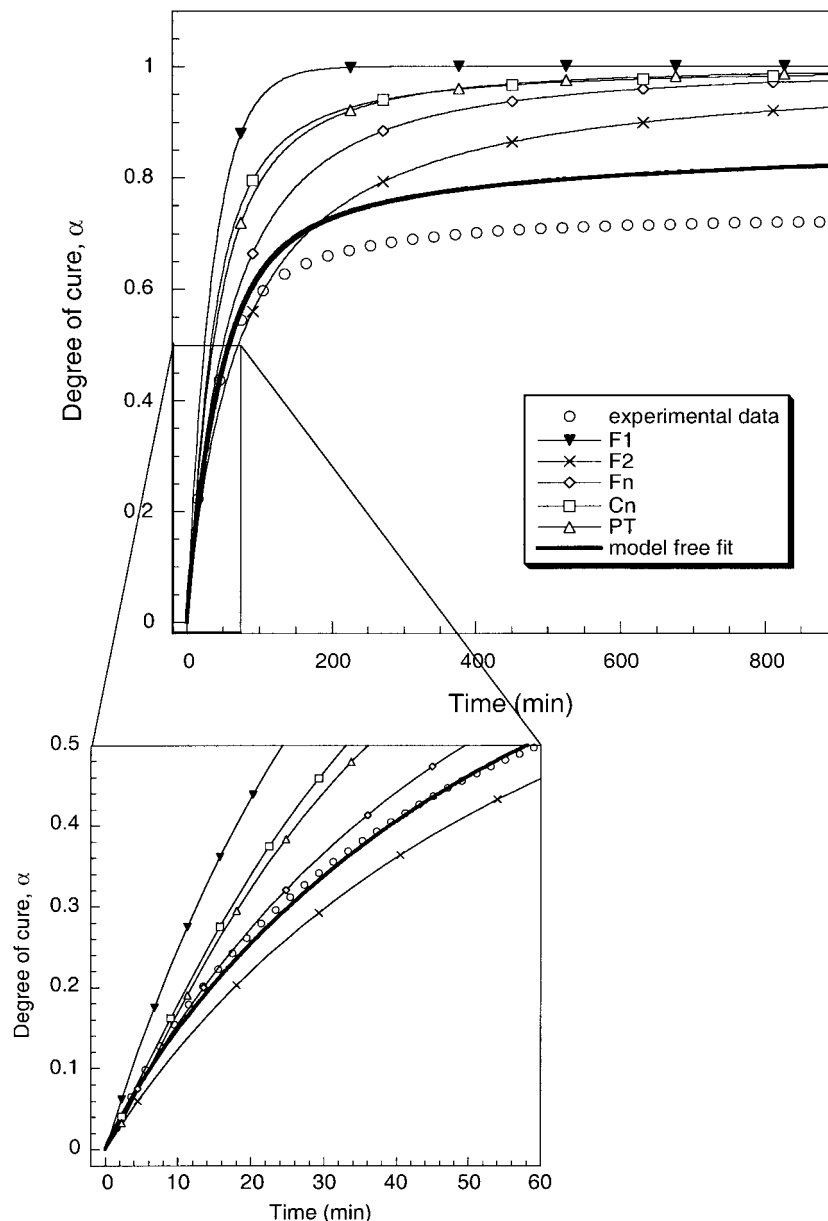


Figure 8. Model predictions for isothermal curing at 30 °C for the case of the medium catalyst concentration overlaid with a 900-min isothermal cure experiment.

A 15th-order polynomial was used to fit the E and $\ln[A \times f(\alpha)]$ data from Figure 6, and together with eq 4, predictions for the cure rate at various heating rates were obtained. Figure 7 shows these model-free predictions compared with the experimental data for the medium catalyst concentration. Excellent agreement is apparent over all of the heating rates investigated.

Model predictions for isothermal curing at 30 °C for the medium catalyst concentration together with the experimental data for a 15-h iso-

thermal cure are plotted in Figure 8. During the first hour of curing, the model-free prediction fits the experimental data extremely well. The major differences between the various kinetic models are readily apparent at longer times. In particular, the model-free prediction suggests that the ultimate degree of cure is significantly lower than that in any of the reaction models because of the increase in activation energy for $\alpha > 0.6$ (see Fig. 6). Although the isothermal model-free fit deviates from the experimental values for degrees of

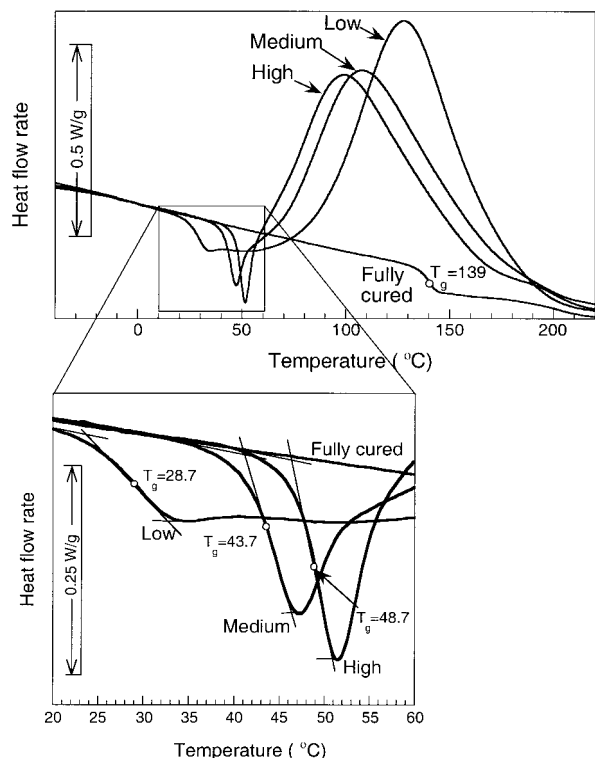


Figure 9. Dynamic scans (15 °C/min) of a fully cured control sample and samples just after the 30 °C/900-min isothermal runs for low, medium, and high concentrations.

cure greater than 0.5 (Fig. 8), it does a much better job of predicting the isothermal cure kinetics than any of the model-fitting approaches.

After the 15-h isothermal cure at 30 °C, these samples were then scanned at 15 °C min⁻¹ from -50 to 220 °C via DSC. These scans for all three catalyst concentrations are shown in Figure 9. Also included in Figure 9 is a dynamic scan at 15 °C min⁻¹ of a fully cured sample (low catalyst concentration), which yields a glass-transition temperature (T_g) of 139 °C. T_g 's after isothermal curing for the low-, medium-, and high-concentration samples are 28.7, 43.7, and 48.7, respectively. It is apparent from the results that further polymerization does not occur until after the sample reaches T_g . One reason for the deviation between the model-free prediction and the isothermal data for degrees of cure greater than 0.5 is the difference in curing conditions. Specifically, the dynamic data on which the model-free fit is based was obtained via curing above T_g , whereas the isothermal data eventually reach conditions in which curing occurs below the glass transition. For the more accurate modeling of the isothermal case at degrees of cure greater than 0.5, a model

that includes the influence of the cure-dependent T_g should be employed.

Another feature of the medium- and high-concentration scans in Figure 9 is the presence of an endothermic peak in the T_g region before the larger exothermic curing peak. Similar endothermic peaks attributed to enthalpic relaxation or physical aging are often seen in glassy polymers as a result of slow cooling through the glass-transition region or annealing below T_g .¹⁸ The annealing time and temperature have a large effect on the position and magnitude of these annealing peaks. For the medium and high catalyst concentrations, the end of the annealing peak is superimposed with the beginning of the exothermic curing peak. Therefore, the measured T_g for these cases slightly overestimates the true T_g . The presence of these superimposed annealing peaks also complicates the measurement of the residual heat of reaction for these cases.

The isothermal model-free predictions for all three catalyst concentrations at 30 °C is shown in Figure 10. The predictions show a significant difference between the low and high concentrations for the time necessary to reach a given degree of cure. For example, the degree of cure for the high catalyst concentration is nearly double that of the low catalyst concentration after 60 min at 30 °C.

CONCLUSIONS

In this work, several reaction models were used to analyze dynamic DSC data for the cure of DCPD

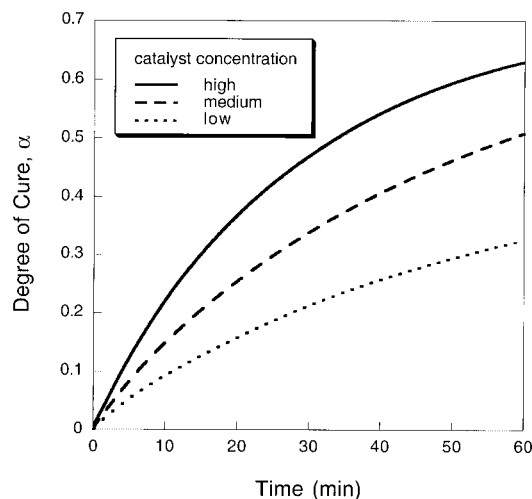


Figure 10. Predictions for isothermal curing at 30 °C based on the model-free isoconversional method for low, medium, and high catalyst concentrations.

with three different concentrations of Grubbs' catalyst. The catalyst concentration had a large effect on the cure kinetics. Of the standard reaction models, the n th-order autocatalytic model performed the best. However, the model-free isoconversional method provided the best fit of the data over the range of heating rates investigated. From the isoconversional method, the activation energy was shown to increase significantly for $\alpha > 0.6$. As a result, the model-free method predicted a lower degree of cure for long periods of time than any of the standard reaction models. This behavior was qualitatively verified by isothermal cure experiments at 30 °C.

APPENDIX: STATISTICAL EVALUATION

The correlation coefficient (r) is defined as

$$r = \sqrt{1 - \frac{\text{LSQ}}{\sum_s \left[\sum_k Y_{s,k}^2 - \left(\sum_k Y_{s,k} \right)^2 / N_s \right]}} \quad (\text{A1})$$

$$\text{LSQ} = \sum_{j=1}^S \sum_{k=1}^{N_s} (Y_{j,k} - \hat{Y}_{j,k})^2 \quad (\text{A2})$$

where $Y_{j,k}$ is the measured value, $\hat{Y}_{j,k}$ is the regress value, S is the number of scans, and N_s is the number of measured values in a particular scan.

The F test compares the residual variances of the individual models against one another. It is used to assess whether there is a statistically significant difference between the models with respect to the quality of fit to the experimental data. The model with the lowest correlation coefficient is typically taken as the reference model. The F -test value is then defined as

$$F_{\text{exp}}(f_1, f_2) = \frac{\sum_{j=1}^s \sum_{k=1}^{N_s} [Y_{j,k} - \hat{Y}_{j,k}(\text{model}_1)]^2 / f_1}{\sum_{j=1}^s \sum_{k=1}^{N_s} [Y_{j,k} - \hat{Y}_{j,k}(\text{model}_2)]^2 / f_2} \quad (\text{A3})$$

where f_1 is the degree of freedom of model 1 and f_2 is the degree of freedom of model 2 (the reference model).¹⁹ F_{exp} is then compared with the critical value of the F distribution, $F_{\text{crit}}(f_1, f_2)$, for a given confidence level. $F_{\text{exp}} < F_{\text{crit}}$ indicates no statisti-

cal difference, whereas $F_{\text{exp}} > F_{\text{crit}}$ indicates that model 1 is significantly better suited for characterization of the experimental data.

The research described in this article was supported by a grant from the Air Force Office of Scientific Research (F49620-00-1-0094) and by a graduate fellowship from the Beckman Institute for Advanced Science and Technology at the University of Illinois at Urbana-Champaign. Thanks are extended to Josh Orlicki for his assistance with and training on DSC and thoughtful discussion. The authors are also grateful to Jeff Moore for his insights and review and to Nancy Sottos, Paul Braun, Eric Brown, and Suresh Sriram for their technical support.

REFERENCES AND NOTES

- Schwab, P.; Grubbs, R. H.; Ziller, J. W. *J Am Chem Soc* 1996, 118, 100–110.
- Macosko, C. W. *RIM, Fundamentals of Reaction Injection Molding*; VCH, New York, 1989.
- White, S. R.; Sottos, N. R.; Geubelle, P. H.; Moore, J. S.; Kessler, M. R.; Sriram, S. R.; Brown, E. N.; Viswanathan, S. *Nature* 2001, 409, 794–797.
- Kessler, M. R.; White, S. R. *Compos A* 2001, 32, 683–699.
- Halley, P. J.; Mackay, M. E. *Polym Eng Sci* 1996, 36, 593–608.
- Borchardt, H. J.; Daniels, F. *J Am Chem Soc* 1957, 79, 41–46.
- Friedman, H. L. *J Polym Sci Part C: Polym Symp* 1963, 6, 183.
- Flynn, J. H.; Wall, L. A. *J Polym Sci Part B: Polym Lett* 1966, 4, 323–328.
- Ozawa, T. *Bull Chem Soc Jpn* 1965, 38, 1881.
- Shin, D. D.; Hahn, H. T. *Compos A* 2000, 31, 991–999.
- Ng, H.; Manas-Zloczower, I. *Polym Eng Sci* 1994, 34, 921–928.
- Vyazovkin, S. *Int J Chem Kinet* 1996, 28, 95–101.
- Pielichowski, K.; Czup, P.; Pielichowski, J. *Polymer* 2000, 41, 4381–4388.
- Cooney, J. D.; Day, M.; Wiles, D. M. *J Appl Polym Sci* 1984, 29, 911–923.
- MacCallum, J. R.; Munro, M. V. *Thermochim Acta* 1992, 203, 457.
- Montserrat, S.; Flaque, C.; Pages, P.; Malek, J. *J Appl Polym Sci* 1995, 56, 1413–1421.
- Montserrat, S.; Andreu, G.; Cortes, P.; Calventus, Y.; Colomer, P.; Hutchinson, J. M.; Malek, J. *J Appl Polym Sci* 1996, 61, 1663–1974.
- McKenna, G. In *Comprehensive Polymer Science*; Booth, C.; Price, C., Eds.; Oxford: New York, 1989; Vol. 2, pp 311–362.
- Netzsch Thermokinetics (v. 2001.2), Statistical Evaluation of Results; 2001 (program help).